# Azafullerene $C_{59}N$, a stable free radical substituent in crystalline $C_{60}$

Ferenc Fülöp [a], Antal Rockenbauer [b], Ferenc Simon [a], Sándor Pekker [c], László Korecz [b], Slaven Garaj [d], András Jánossy [a,*]

[a] *Budapest University of Technology and Economics, Institute of Physics, POB 91, Budapest H-1521, Hungary*
[b] *Chemical Research Center, Institute of Chemistry, POB 17, Budapest H-1525, Hungary*
[c] *Research Institute for Solid State Physics and Optics, POB 49, Budapest H-1525, Hungary*
[d] *Ecole Polytechnique Federale de Lausanne, Institut de Genie Atomique, CH-1015 Lausanne, Switzerland*

Received 18 September 2000; in final form 6 November 2000

## Abstract

Solid solutions of $C_{59}N$ azafullerene in $C_{60}$ with concentrations of $10^{-5}$ to $10^{-4}$ were produced in large quantities in an electric gas discharge tube. $C_{59}N$ is a stable monomeric substituent molecule in crystalline $C_{60}$. The isotropic $^{14}N$ and $^{13}C$ hyperfine coupling constants measured by electron spin resonance (ESR) are characteristic of the extent of delocalization of the charge over the cage and are a sensitive test of electronic structure calculations. The $C_{59}N$ reorientational activation energy measured below the face centered cubic (fcc) to simple cubic (sc) transition is 2300 K. This value is similar to that of the matrix $C_{60}$ molecules, indicating that $C_{59}N$–$C_{60}$ intermolecular interactions are weak. © 2001 Elsevier Science B.V. All rights reserved.

Azafullerene, $C_{59}N$, is one of the most interesting chemical modifications of the fullerene $C_{60}$. In this molecule an unpaired electron is added to the lowest unoccupied molecular orbital by substituting a carbon atom for a nitrogen atom (Fig. 1). The resulting structure carries magnetic and electric dipole moments and is only slightly deformed [1]. The synthesis in bulk quantities by Hummelen et al. [2] showed that the solid consists of $(C_{59}N)_2$ dimers. The structural and electronic properties of the dimer have been studied in detail [3]. On the other hand, dimerization has been a major obstacle to the study of monomeric $C_{59}N$ and although several calculations of the electronic and molecular structure of $C_{59}N$ were published [3], the extent of delocalization of the charge over the cage could not be measured as the monomer was not available in sufficient amounts. There are various ways to obtain minute quantities of the monomeric radical. The formation of $C_{59}N$ using $N^+$ ion bombardment of evaporated $C_{60}$ was observed in the mass spectrum by Christian et al. [4]. A weak electron spin resonance (ESR) of the monomer was observed using photolysis of $(C_{59}N)_2$ in solutions [5,6] and thermal homolysis [7] in solid $(C_{59}N)_2$. A few molecular layers of monomers were obtained [8,9] by sublimation of $(C_{59}N)_2$.

In this Letter we describe a simple way to produce solid solutions of $C_{59}N$ in $C_{60}$ ($C_{59}N:C_{60}$) in

* Corresponding author. Fax: +36-1-463-3819.
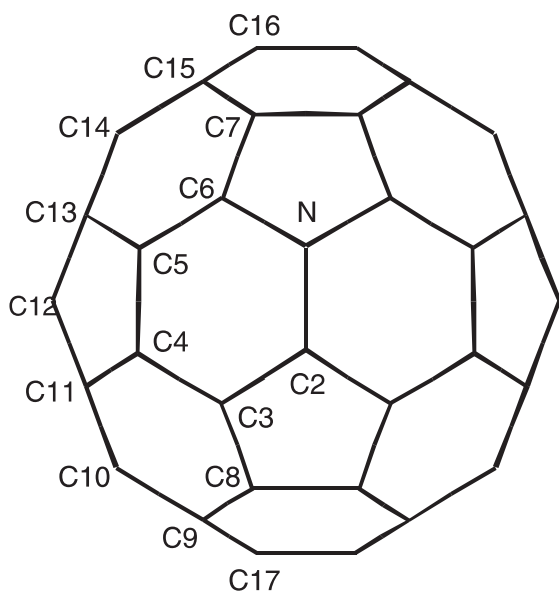*E-mail address:* atj@power.szfki.kfki.hu (A. Jánossy).

Fig. 1. The $C_{59}N$ molecule. Calculated isotropic hyperfine constants (in mT) are $^{14}N$: 0.87, $^{13}C2$: +2.29, $^{13}C3$: −0.80, $^{13}C4$: +0.88, $^{13}C10$: 0.44 , all other $^{13}C$: less than 0.4.

an electric gas discharge tube. We find that monomeric $C_{59}N$ is stable in this solid solution and its rotational dynamics parallels that of $C_{60}$ in the bulk. The production of $C_{59}N$:$C_{60}$ in large quantities allowed us to measure the various $^{14}N$ and $^{13}C$ hyperfine constants that are a sensitive test of electronic structure calculations.

We produced $C_{59}N$ in a $N_2$ gas discharge tube originally designed for the production of endohedral $N@C_{60}$ following the method of Pietzak et al. [10]. Typical experimental conditions were: 1 mb $N_2$ pressure, 1 mA discharge current, 10 cm electrode distance. The tube is heated to about 540°C at one electrode (usually the anode) while the other electrode is water-cooled and is at ambient temperature. $C_{60}$ powder placed between the electrodes at the bottom of the tube is sublimed and deposited onto the wall of the quartz tube and the cooled electrode. As the electric discharge is turned on, $N^+$ ions in the plasma react with $C_{60}$ to form $N@C_{60}$ and $C_{59}N$ simultaneously. Endohedral $N@C_{60}$ is collected from the water-cooled electrode but is produced in the gas phase and not in $C_{60}$ deposited onto the wall. Attempts were unsuccessful to 'implant' $N^+$ ions into a layer de-

posited onto the cold surface before the electric discharge was turned on. $C_{59}N$:$C_{60}$ is collected from the heated surface of the quartz tube. The highest concentration of $C_{59}N$ in $C_{60}$ of about 100 ppm (determined from the ESR intensity) was found in a narrow stripe on the quartz tube in the hottest region where deposition still occurred, i.e. where the temperature is roughly 400°C. $C_{59}N$ accumulates in the high temperature region, probably because the vapor pressure of $C_{59}N$ is lower than that of $C_{60}$. The yield of $C_{59}N$:$C_{60}$ (with concentration of 100 ppm) is about 5% of the starting $C_{60}$ material. After deposition, the discharge tube was opened to air before sealing the samples into quartz tubes under helium. The material is stable in He atmosphere. In air, $C_{59}N$ decays at ambient temperatures in about a week. X-ray diffraction showed that the deposited powder mainly consists of crystalline $C_{60}$. The ESR spectrum shows a low concentration of unknown free radicals formed during the production. We have not attempted to purify the material.

Electron spin resonance (ESR) was performed at 9 GHz (X-band), 75 and 225 GHz. We identified the material as a solid solution of $C_{59}N$ in $C_{60}$ from the similarity of the ESR spectrum to that of monomers produced by photo or thermolysis. At 300 K (Fig. 2) the three $^{14}N$ ($I=1$) hyperfine lines characteristic of rapidly tumbling free radicals are observed with $g_{av} = 2.0014(2)$ and an isotropic hyperfine coupling constant, $A_{iso} = 0.363(1)$ mT. These values are very close to $g_{av} = 2.0013$ and $A_{iso} = 0.373$ mT of [5] and $g_{av} = 2.0011(1)$ and $A_{iso} = 0.37$ mT [6] for $C_{59}N$ induced by photolysis in chloronaphtalene solution. The thermally induced monomer [7] in solid $(C_{59}N)_2$ has nearly the same hyperfine constant $A_{iso} = 0.360(1)$ but a somewhat smaller g value, $g_{av} = 2.0004(2)$.

The ESR spectrum is temperature independent between 257 and 290 K. As shown in Fig. 2, the spectrum consists of narrow $^{14}N$ hyperfine lines with widths limited by instrumental resolution (0.012 mT at 9 GHz) and a series of well resolved $^{13}C$ lines. In this temperature range the $C_{59}N$ molecules are rapidly reorienting in all three directions together with the $C_{60}$ molecules of the matrix. The reorientation is fast on the time scale of the ESR measurement and all anisotropic
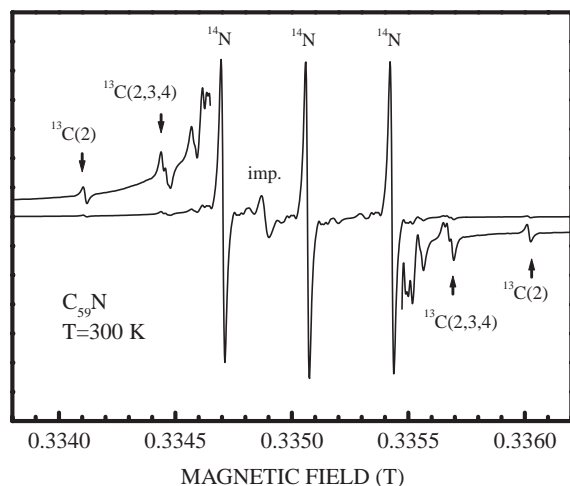
Fig. 2. Motionally narrowed ESR spectrum of tumbling $C_{59}N$ substituted in $C_{60}$ at 290 K and 9 GHz. Wings are 10 times magnified. The outmost lines correspond to site C2, (with $^{14}N$ nuclear spin states $m = \pm 1$) the next lines are a superposition from hyperfine lines of sites C2 ($m = 0$), C3 and C4 ($m = \pm 1$), as defined in Fig. 1. An unidentified impurity line is denoted by 'imp'. Other lines are unassigned $^{13}C$ lines.

interactions are averaged to zero. The motional narrowing of the ESR spectrum of the rapidly reorienting $C_{59}N$ molecule remains effective even at high ESR frequencies where relaxation due to *g*-factor anisotropy is more important. At 290 K and 225 GHz the linewidth was less than the instrumental resolution of 0.05 mT.

Table 1 shows the measured $^{13}C$ isotropic hyperfine coupling constants determined by a computer fit to the spectrum at ambient temperature and X-band. Isotropic Fermi contact couplings were calculated by the density functional ab initio method, B3LYP with 6-31G* basis set on a PM3

Table 1
Measured $^{13}C$ isotropic hyperfine constants

| $A_{iso}$ (mT) | Number of sites |
|---|---|
| 1.180 | 1 |
| 0.518 | 2 |
| 0.484 | 2 |
| 0.258 | 2 |
| 0.230 | 2 |
| 0.166 | 4 |
| 0.134 | 4 |
| 0.11 | 6 |

optimized molecular geometry of $C_{59}N$. The calculations were carried out using the GAUSSIAN 98 software [11]. The results for sites around the N atom are given in the caption of Fig. 1. The electronic structures of the monomer and the dimer forms of $C_{59}N$ were determined previously by Andreoni et al. [1,12,13] applying a similar method.

The agreement between calculated and measured hyperfine constants is not particularly good. In the computer fit the numbers of sites contributing to the resolved $^{13}C$ lines (Table 1) were left as free parameters. $C_{59}N$ has a $C_S$ symmetry with a single mirror plane given by the N atom, the C2 site and the center of the cage (Fig. 1). There are 31 inequivalent C sites, 3 'single' sites and 28 sites with chemically equivalent pairs. (In Table 1 site numbers more than 2 indicate unresolved, chemically different sites.) The $^{13}C$ line with the largest coupling (1.180 mT) arises from a single carbon atom. This unambiguously assigns it to C2, the nearest neighbor to N site in the symmetry plane. The other two single sites are unlikely to be resolved. According to the calculation, the spin density does not decrease monotonically with the distance from N. The relatively close N neighbors, C3 and C4 have coupling constants with similar magnitudes but opposite signs. This indicates that the $^{13}C$ lines with measured coupling constants of 0.518 and 0.484 mT correspond to these sites. (We cannot measure the sign of coupling constants.) The extra spin density is not well localized to the first C neighbors of N as 23 of the 59 carbon atoms have 10% or larger spin density than the N first neighbor C2 site (Table 1).

Pure $C_{60}$ has a first-order phase transition at 261 K from a low temperature simple cubic (sc) to the high temperature face centered cubic (fcc) structure with a small change in the volume [14]. In the sc structure $C_{60}$ molecules have two inequivalent orientations with respect to the crystal axes. At low temperatures the molecular orientations are arranged preferentially in two standard configurations with respect to each other. There is a merohedral disorder of regions with differing configurations. As the temperature is raised, molecules fluctuate more and more rapidly between the possible orientations with large angle jumps. The orientational correlation time, $\tau$, is activated

$$\tau = \tau_0 \exp\{T_0/T\}. \tag{1}$$

$\tau_0(C_{60}) \approx 5 \times 10^{-15}$ s and $T_0(C_{60}) = 2980$ K were obtained [15] from $^{13}$C nuclear spin–lattice relaxation in bulk $C_{60}$. In the high temperature fcc phase reorientation proceeds with small angle rotations and $C_{60}$ molecules may be oriented in all directions. In the following we show that the dynamics of $C_{59}N$ follow closely that of bulk $C_{60}$. We deduce $\tau(C_{59}N)$ from the electronic spin lattice and spin–spin relaxation rates $T_1^{-1}$ and $T_2^{-1}$, respectively.

The low temperature ESR spectra at 9 and 75 GHz are shown in Fig. 3. At this temperature the structure is static on the scale of the inverse frequency spread, $1/\Delta\omega_0$ ($\sim 10^{-8}$ s at X-band) due to the anisotropic interactions. The spectra were fitted with the simplifying assumptions that the principal axes of the hyperfine and $g$ factor anisotropy tensors coincide and that these tensors have no distribution due to the disorder in the orientation of $C_{59}N$ with respect to neighboring $C_{60}$ molecules. The corresponding parameters are listed in the caption of Fig. 3. The fit reproduces the main features of the spectra but is not perfect. Differences between values obtained at 9 and 75 GHz are indicative of the accuracy possible with the above-mentioned simplifications. At low temperatures the spectrum is broad and the impurity line has a large amplitude. In Fig. 3 the calculated spectra represent fits to the experimental data with the impurity line substracted for clarity.

Fluctuations of the anisotropy of the $g$-factor and hyperfine fields at tumbling molecules determine $T_1^{-1}$. In general: $T_1^{-1} = C^2\tau/(1 + (\omega_0\tau)^2)$, where $C^2$ is proportional to the time averaged squared local field at the N atom and $\omega_0$ is the Larmor frequency. We measured $T_1^{-1}$ at 9 GHz between 135 and 205 K using the saturation of the ESR line amplitude as a function of microwave power. The data show that $\omega_0\tau \gg 1$ in the above temperature range thus $\tau \propto T_1$. We find an activated $T_1$ with $T_0(C_{59}N) = 2240$ K.

Above 210 K the 9 GHz static spectrum transforms into the isotropic spectrum of three hyperfine components with strongly temperature dependent linewidths. The broadening depends on the nuclear spin state, $m$ and is largest for the low
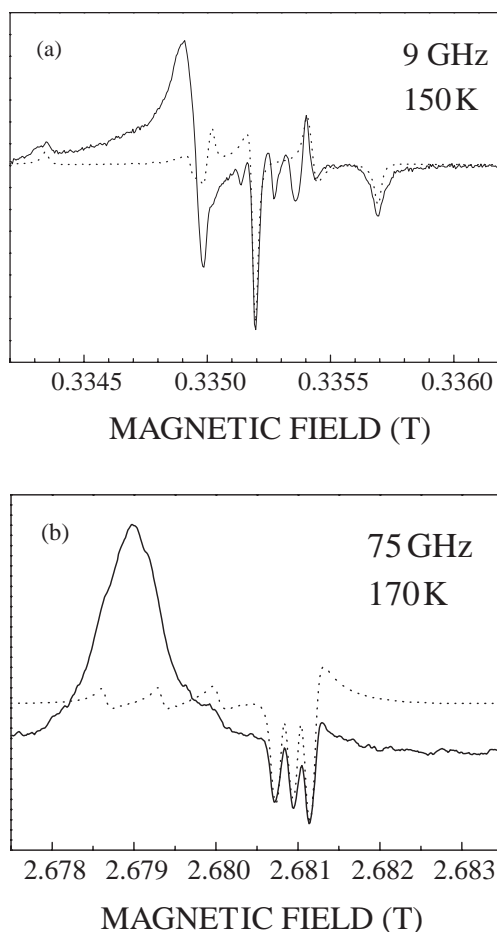




Fig. 3. ESR spectra of static $C_{59}N$ at (a) 9 GHz and 150 K, (b) 75 GHz and 170 K. Continuous line: experiment, dotted line: fit. Fit parameters: (a) $g_{xx} = 2.00109$, $g_{yy} = 2.00116$, $g_{zz} = 2.00214$, $A_{xx} = 0.21$, $A_{yy} = 0.25$, $A_{zz} = 0.67$ mT. (b) $g_{xx} = 2.00106$, $g_{yy} = 2.00113$, $g_{zz} = 2.00230$, $A_{xx} = 0.21$, $A_{yy} = 0.20$, $A_{zz} = 0.68$ mT. Lines at $0.3349T$ and $2.679T$ in (a) and (b), respectively are due to impurities.

field transition, $m = 1$. These features are a nice example of motional narrowing of the static spectrum that occurs for $\Delta\omega_0\tau < 1$. In this regime the lineshapes are Lorentzian with half width $\Delta H = 1/(\gamma T_2)$. The widths of the hyperfine components are proportional to the correlation time, $1/T_2 = K(m)\tau$. In general the constants, $K(m)$, depend on the $g$-factor and hyperfine anisotropy. $1/T_2$ follows an activated behavior between 210 and 257 K with $\Delta E_{C_{59}N}/k_B = 2400$ K.
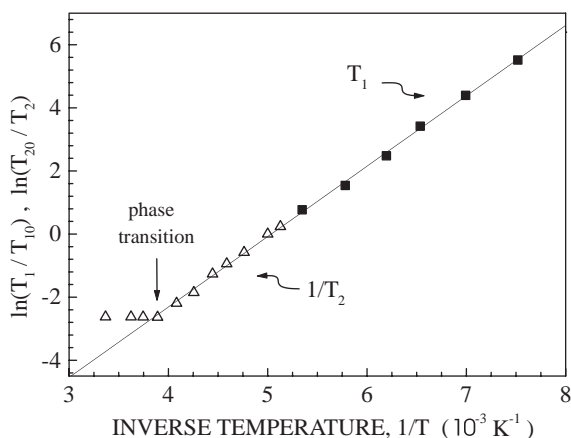
Fig. 4. ln $T_1$ and ln $T_2$ vs. $1/T$. The spin lattice relaxation time, $T_1$, and above 200 K, the transverse spin relaxation rate $T_2^{-1}$ are proportional to the rotational correlation time of $C_{59}N$, $\tau(C_{59}N)$. The data are normalized to the relaxation times $T_{10}$ and $T_{20}$ measured at 200 K. The line is a linear fit to ln$\tau$ with an activation energy of $\Delta E_{C_{59}N} = 2300$ K .

The activation energies measured from $T_1$ and $1/T_2$ are equal within experimental precision. In Fig. 4 we fit the full set of $T_1$ and $1/T_2$ data (normalized to 200 K) with a single energy, $\Delta E_{C_{59}N}/k_B = 2300$ K. We find $\tau_0(C_{59}N) \approx 10^{-13}$ s by assuming $\Delta\omega_0\tau = 1$ at 200 K, i.e. at the temperature of the collapse of the static spectrum.

The value of $\Delta E_{C_{59}N} = 2300$ K is remarkably close to $\Delta E_{C_{60}} = 2980$ K, the activation energy of the correlation time of the rotation of $C_{60}$ molecules measured [15] in pure $C_{60}$. The close agreement between $\Delta E_{C_{59}N}$ and $\Delta E_{C_{60}}$ indicates that the reorientation dynamics of $C_{59}N$ follows that of the bulk. This would not be so if interactions between $C_{59}N$ and $C_{60}$ were strong. For example in $RbC_{60}$ the $C_{60}$ ions spontaneously form covalent bonds when their rotation is sufficiently slow [16].

In summary, $C_{59}N$ is a stable substituent molecule in $C_{60}$ crystals at all temperatures below the formation of the solid solution at 400°C. The impurity state of $C_{59}N$ does not overlap appreciably with neighboring $C_{60}$ molecules and rotational dynamics are similar. Hyperfine interactions of the free radical with $^{14}N$ and $^{13}C$ show a partial delocalization of the extra electron over the cage.

## Acknowledgements

## References

[1] W. Andreoni, F. Gygi, M. Parrinello, Chem. Phys. Lett. 190 (1992) 159.

[2] J.C. Hummelen, B. Knight, J. Pavlovich, R. Gonzalez, F. Wudl, Science 269 (1995) 1554.

[3] See the review by J. C. Hummelen, C. Bellavia-Lund, F. Wudl Heterofullerenes, in: Topics in Current Chemistry, vol. 199, Springer, Berlin, Heidelberg, 1999, p. 93 (and references therein).

[4] J.F. Christian, Z. Wan, S.L. Anderson, J. Phys. Chem. 96 (1992) 10597.

[5] K. Hasharoni, C. Bellavia-Lund, M. Keshavarz-K, G. Srdanov, F. Wudl, J. Am. Chem. Soc. 119 (1997) 11128.

[6] A. Gruss, K.-P. Dinse, A. Hirsch, B. Nuber, U. Reuther, J. Am. Chem. Soc. 119 (1997) 8728.

[7] F. Simon, D. Arcon, N. Tagmatarchis, S. Garaj, L. Forró, K. Prassides, J. Phys. Chem. A. 103 (1999) 6969.

[8] M.J. Butcher, F.H. Jones, P.H. Beton, P. Moriarty, B.N. Coteir, M.D. Upward, K. Prassides, K. Kordatos, N. Taamatardaic, F. Wudl, V. Dhanak, T.K. Johal, C. Crotti, C. Comicioli, C. Ottaviani, Phys. Rev. Lett. 83 (1999) 3478.

[9] Ch. Sommerhalter, B. Pietzak, M.Ch. Lux-Steiner, B. Nuber, U. Reuther, A. Hirsch, Surf. Sci. 433 (1999) 486.

[10] B. Pietzak, M. Waiblinger, A.T. Murphy, A. Weidinger, M. Höhne, E. Dietel, A. Hirsch, Chem. Phys. Lett. 279 (1997) 259.

[11] GAUSSIAN 98, Revision A.7, Gaussian, Inc., Pittsburgh, PA, 1998.

[12] W. Andreoni, A. Curioni, K. Holczer, K. Prassides, M. Keshavarz-K, J.-C. Hummelen, F. Wudl, J. Am. Chem. Soc. 118 (1996) 11335.

[13] W. Andreoni, A. Curioni, in H. Kuzmany, J. Fink, M. Mehring, S. Roth, (Eds.) Proc. IWEPNM 1996, World Scientific, Singapore, p. 359.

[14] P.A. Heiney, G.B.M. Vaughan, J.E. Fischer, N. Coustel, D.E. Cox, J.R.D. Copley, D.A. Neumann, W.A. Kanitakahara, K.M. Creegan, D.M. Cox, J.P. McCauley, A.B. Smith, Phys. Rev. B 45 (1992) 4544.

[15] K. Mizoguchi, Y. Maniwa, K. Kume, Mater. Sci. Eng. B 19 (1993) 146.

[16] S. Pekker, L. Forró, L. Mihaly, A. Jánossy, Solid State Commun. 90 (1994) 349.